5th SASTech
Iran | Mashhad
May 12 - 17 | 2011
5th Symposium on Advances in Science & Technology

Comparison of Multimode Interference Couplers: Gaussian-mode and Sinusoidal-mode Cases

A. Mahmoodi[1], M. Tajaddini[2]
[1]Sama Technical and Vocational Training College,
Islamic Azad University, Karaj Branch, Karaj, Iran
Email:omid.phy@gmail.com
[2] Islamic Azad University, Baft Branch, Baft, Iran
Paper Reference Number: 1312-420
Name of the Presenter: A. Mahmoodi

Abstract

Analysis of the multimode-interference couplers can be done by using the sinusoidal eigen-modes and also the Gaussian eigen-modes for the multimode region. Study of the multimode interference couplers using the sinusoidal eigen-modes is based on the self-imaging concept of the multimode waveguides. These modes can be determined by using the planar waveguide theory. In Gaussian model, eigen-modes of the multimode region are obtained by using the Gaussian mode theory. In this paper, direct comparison of the multimode interference couplers with Gaussian eigen-modes and couplers with sinusoidal eigen-modes is done. The coupling coefficients of the field for these models are compared. In addition, a comparison is made between wave propagation analysis of Gaussian model and wave propagation simulation by FEMLAB software and FDTD method for MMI couplers with ultrashort lengths. It is shown that the Gaussian model results, unlike the sinusoidal model, are in good agreement with the simulation results. In other words, the Gaussian model is necessary for analysis of the ultrashort MMI couplers and also the sinusoidal model is not suitable for small lengths. In fact, building-up of the sinusoidal modes is the result of multiple interference of the reflected waves that appears in larger lengths. In addition, for long MMI couplers, the Gaussian modes are gradually transformed into the sinusoidal modes and the results of the sinusoidal model with self-imaging principle is true to handle these types of devices.

Key words: MMI coupler, multimode interference, sinusoidal mode, Gaussian mode, self-imaging

1. Introduction

In the past decade, multimode interference (MMI) coupling devices [Soldano, L.B. & Pennings, E.C.M. (1995)] have become important components in photonic and optoelectronic integrated circuits. In fact, unique properties of MMI couplers such as simple structure, low loss, low polarization sensitivity, large optical bandwidth, compact size and good fabrication tolerances make them attractive components for integration in more complex and advanced photonic integrated circuits. Already, MMI couplers have been applied as optical power splitters and combiners, optical filters, optical switches and Mach-Zehnder switches. An MMI coupler essentially consists of three parts; a wide multimode waveguide region, a single or set of access waveguides (input and output waveguides). It is usually assume that the access waveguides support only one mode. There are a number of analytical and numerical approaches to modeling the MMI coupler

such as, guided-mode propagation analysis (MPA) [Soldano, L.B. & Pennings, E.C.M. (1995)], ray optics method [Ulrich, R. & Ankele, G. (1975)], hybrid methods [Chang, D. C. & Kuester, E. F. (1981)], and BPM type simulations. The analytical approaches in comparison with numerical approaches have advantages, which in addition are basis for design and numerical approaches; it is also provide some insight into the operation of the MMI devices. It should be noted to simplify the analytical method some assumptions usually are made. These assumptions produce a lack of accuracy to some degree. In this paper, we compare two analytical methods, i.e., sinusoidal and Gaussian models, to modeling the guiding region of the MMI couplers. For Gaussian model the Gaussian mode field amplitude [Mahmoodi, A. et al. (2009)] and for sinusoidal model the sine-like mode field amplitude [Soldano, L.B. & Pennings, E.C.M.(1995)] is approximated.

2.Multimode interference coupler

The Fig. 1 shows a geometry structure of the 2×2 MMI coupler, where L_{MMI} and W_{MMI} are the length and width of the multimode interference region, respectively. The effective refractive index of the MMI region is equal to n_1 and the effective refractive index of the cladding region is assumed to be n_2.

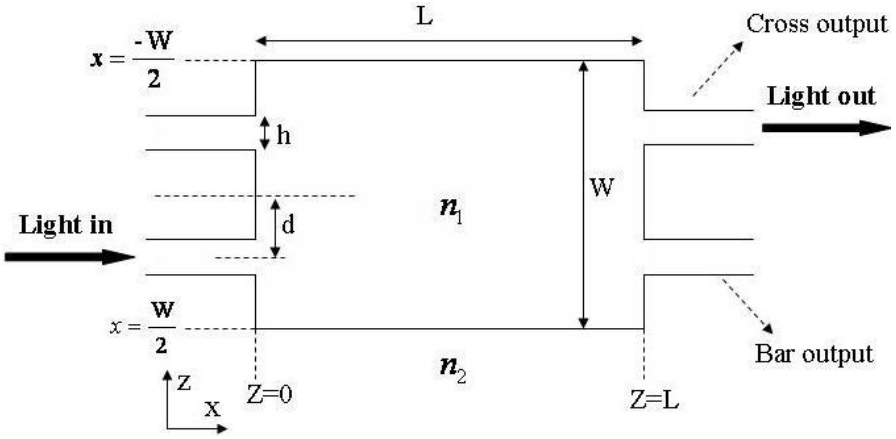

Fig. 1: A schematic structure of the 2×2 MMI coupler.

When the transverse dimensions of MMI waveguide are much larger than the lateral dimensions, we can assume that the modes have the same lateral behavior everywhere in the waveguide. In this case, we can neglect this dimension and therefore analysis of the waveguide without losing generality is done by using a two-dimensional structure, that is, transverse and longitudinal dimensions. In fact, by using the effective index method (EIM) [Izuka, K. (2002)] a 2-D structure can be obtained from the 3-D physical multimode waveguide. When an input light, which has the profile of the input waveguide mode, reaches the input facet of the MMI region (supports *m* guided and radiative modes) it causes excitation of the several modes of that region. Thus, at $z = 0$ we have

$$\psi(x,0,t) = \sum_{\nu} c_{\nu,d}\,\varphi_{\nu,d}(x,0,t) \quad , \tag{1}$$

Where $\varphi_\nu(x,z,t) = \varphi_\nu(x,z)\exp(j\omega t)$ is the ν^{th} mode of the MMI region and c_ν is the excitation coefficient of the ν^{th} mode.

3.Theory of the Sinusoidal model

3.1. The sinusoidal modes

The field distribution in the multimode region can be stated in terms of the sinusoidal guided modes of that region:

$$\psi(x,z,t)=\sum_{\nu=0}^{m-1}c_\nu\varphi_\nu(x,z,t)=\sum_{\nu=0}^{m-1}c_\nu\varphi_\nu(x)\exp[\,j(\omega t-\beta_\nu z)] \tag{2}$$

The propagation constants must satisfy the following dispersion equation

$$k_{x,\nu}^2+\beta_\nu^2=n_1{}^2k_0^2 \quad , \tag{3}$$

where $k_0=2\pi/\lambda_0$ and λ_0 is the free space wavelength, $k_{x,\nu}$ and β_ν are the transverse and longitudinal propagation constants, respectively. By considering the penetration depth and therefore the Goos-Hänchen phase shift [Marcuse, D. (1974)] of each mode at boundaries, we have the effective wide for MMI region [Soldano, L.B. & Pennings, E.C.M. (1995)] as

$$W_e=W+(\lambda_0/\pi)(n_2/n_1)^{2\sigma}(n_1{}^2-n_2)^{-1/2} \quad , \tag{4}$$

($\sigma=0$ for TE and $\sigma=1$ for TM polarization). The transverse propagation constant is determined from the wavelengths of the MMI modes (transverse propagation constant of planar waveguide)[Soldano, L.B. & Pennings, E.C.M. (1995)] as

$$k_{x,\nu}=\pi(\nu+1)/W_e \quad . \tag{5}$$

Setting of Eq. 5 into Eq. 3 yields

$$\beta_\nu=[n_1^2k_0^2-(\pi(\nu+1)/W_e)^2]^{1/2} \quad . \tag{6}$$

By using the first term of the Taylor expansion of Eq. 6 we have

$$\beta_\nu\approx n_1k_0-\frac{(\nu+1)^2\pi\lambda_0}{4n_1W_e{}^2} \quad . \tag{7}$$

The beat length of the two lowest-order modes is defined as

$$L_\pi=\frac{\pi}{\beta_0-\beta_\nu}\approx\frac{\nu(\nu+2)}{3L_\pi} \quad . \tag{8}$$

Therefore, the transverse field profile can be written as

$$\psi(x,z)\approx\sum_{\nu=0}^{m-1}c_\nu\varphi_\nu(x)\exp[\frac{j(\nu+2)\pi}{3L_\pi}z] \quad . \tag{9}$$

3.2. The Self-imaging property

In sinusoidal model, analysis of the MMI coupler is usually studied using the self-imaging concept of multimode waveguide [Soldano, L.B. & Pennings, E.C.M. (1995)]. This property which is related to the interference of the several modes in MMI region is stated when an input field is launched into multimode waveguide is reproduced in single or multiple images at periodic space along the length of the waveguide. In other words, the interference of sinusoidal eigen-modes of the multimode region causes the construction of one or more images at periodic intervals along the propagation direction of the region. There are two mechanisms to study of self-imaging concept of the MMI region, General imaging and Restricted imaging. In general imaging, there is no restriction on the excitation of the modes and interference of the modes is independent of the modal excitation. In this mechanism, single and multiple images under certain conditions are reproduced. For single images, $L=p(3L_\pi)$ and $p=0,1,2,\ldots$. It must be noted that for even modes we have even symmetry and direct images and for odd modes we have odd symmetry and mirrored images. Also, for multiple images $L=p/2(3L_\pi)$ and $p=1,3,5,\ldots$.

In Restricted Imaging, only some of the guided modes in the multimode waveguide are excited by the input fields. This mechanism is classified to paired imaging and symmetry imaging. In paired imaging case, the guided modes which satisfy the $\mathrm{mod}_3[\nu(\nu+2)]=0 \quad (\nu\neq 2,5,8,\ldots)$ will be excited. Therefore, direct and inverted

images of the input light replicated at $L = p(L_\pi)$ and $p = 0,1,2,\ldots$. In symmetry imaging, only guided modes which satisfy $\mathrm{mod}_4[\nu(\nu+2)] = 0$ ($\nu = even$) will be excited and single images of input light will be replicated at $L = p(3L_\pi/4)$ with $p = 0,1,2,\ldots$.

4. Theory of the Gaussian model

In this section, we consider the multimode interference coupler by using a model based on the Gaussian mode theory [Davis, C.C. (1996)] of the MMI region. In this model, which is suitable for ultrashort MMI length [Mahmoodi, A. et al. (2009)], the field distribution in the MMI region can be expressed in terms of the Gaussian modes of that region. As we have also mentioned before, due to small size of the coupler along the transverse dimension (i.e., in the *y* direction), we can therefore eliminate the calculations on that direction. Also, it is assumed that the light field propagates along the *z* axis with slow-varying envelope. For one of these mode (i.e., $\varphi(x,z,t) = \varphi(x,z)\exp(j\omega t)$), by solving the wave equation of the MMI region [Davis, C.C. (1996)] the spatial profile of this mode can be obtained as follows [Mahmoodi, A. et al. (2009)]:

$$\varphi(x,z) = \varphi_0\left(\frac{w_0}{w(z)}\right)^{1/4}\exp\left[\frac{-x^2}{w^2(z)}\right]\exp\left[-j\beta z + \frac{j}{2}\arctan\left(\frac{z}{z_0}\right)\right]\exp\left[\frac{-j\beta x^2}{2R(z)}\right] \quad . \tag{10}$$

Here, all of the parameters are defined similar to the free-space Gaussian modes [Davis, C.C. (1996)]. It must be noted that, for MMI coupler with small lengths, we can ignore the second term of the longitudinal phase factor and the spherical phase factor in Eq.10. As the light field enters the MMI region through the input waveguides (at z=0 in Fig. 1) a continuum of Gaussian modes, each of which propagates along a distinct angle of θ (by $0 < |\theta| < \pi/2$) are excited. To find the profile of an arbitrary mode with an arbitrary θ angle, a local coordinate system (x', z') for the mode is considered (i.e., $z' = z\cos\theta - x\sin\theta$ and $x' = z\sin\theta + x\cos\theta$, $k_{z,\theta} = \beta\cos\theta$ and $k_{x,\theta} = -\beta\sin\theta$). It is assumed that the mode propagates along the z' axis and the angle between z' and *z* axes is θ. Therefore, the mode $\varphi_{\theta,\pm d}(x,z)$ which has the angle θ and starts from $x = \pm d$ is:

$$\varphi_{\theta,\pm d}(x,z) = \varphi_{0,\theta}\left\{\left(\frac{w_0}{w(z)}\right)^{1/4}\exp\left[\frac{-(z\sin\theta + (x\mp d)\cos\theta)^2}{w^2(z)}\right]\right\}\exp\left[-j\beta\left(z\cos\theta - (x\mp d)\sin\theta\right)\right]. \tag{11}$$

All of the excited modes propagate through the MMI region and reflect from the sidewalls of the MMI region. To include the reflections of each mode with angle θ from a wall we can add another Gaussian wave with the angle $-\theta$ from a proper position. For example, for a Gaussian mode with angle θ which starts from the position $x = d$, the reflected wave which at first is reflected form the "right(r) or left (l)" wall (from the position $x = W - d$ or $x = -W - d$) and has "q" reflection(s) is denoted as $\varphi_{\theta,d,r,q}(x,z)$ or $\varphi_{\theta,d,l,q}(x,z)$ .So, the total field distribution along the length of MMI region is given by:

$$\begin{aligned}\psi(x,z) &= \sum_{\theta,q}\left(c_{\theta,d,r,q}\varphi_{\theta,d,r,q}(x,z) + c_{\theta,d,l,q}\varphi_{\theta,d,l,q}(x,z)\right.\\ &= \sum_{\nu}\left(c_{\nu,d}\varphi_{\nu,d}(x,z)\right.\end{aligned} \tag{12}$$

where $\varphi_{\nu,d}(x,z)$ is the ν^{th} Gaussian mode which starts from the position $x = +d$ and includes all of the reflections from the walls. In other words, the Gaussian mode prior to the reflection is as $\varphi_{\nu,d}(x,z) = \varphi_{\theta,d}(x,z)$ and after the reflection is as follows:

$$\varphi_{v,d}(x,z) = (s_{\theta,r})^q \varphi_{\theta,d,r,q}(x,z) + (s_{\theta,l})^q \varphi_{\theta,d,l,q}(x,z) \qquad (13)$$

where $s_{\theta,r(l)}$ is the (Fresnel) coefficient for the reflected mode . Also, the Goos-Hänchen phase shift caused by the total internal ref lection ((is shown in Fig. 2) of the field for MMI couplers is considered. The penetration depth of each Gaussian-mode field in

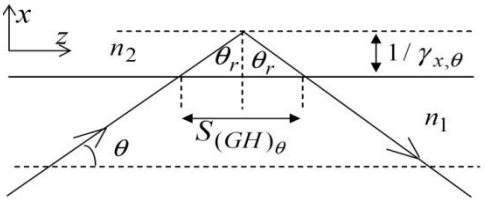

Fig. 2: The total internal ref lection in MMI waveguide. $S_{(GH)_\theta}$ is the Goos-Hänchen phase shift and $1/\gamma_{x,\theta}$ is the penetration depth corresponding to the θ mode.

cladding region is equal to the inverse of the decay constant of the mode in that region. So, The Goos-Hänchen shift can be determined as follows:

$$S_{(GH)_\theta} = \frac{2Tan\theta_r}{\gamma_{x,\theta}} = \frac{2Tan(\pi/2-\theta)}{\gamma_{x,\theta}} \qquad (14)$$

where $\delta_\theta = 1/\gamma_{x,\theta}$ is penetration depth of mode θ, $\theta_r = \pi/2 - \theta$ is reflection angle and $\gamma_{x,\theta}$ is the decay constant of the mode θ. In fact, the decay constant is the propagation constant of the field in cladding layer (evanescent wave).

The reflected mode $\varphi_{\theta,d,r(l),i}(x,z)$ can be obtained by evaluating $X_{r(l)}$ and $Z_{r(l)}$ (corresponding to *x* and *z* in Eq. (3))

$$\varphi_{\theta,d,r(l),i}(x,z) = \varphi_{0,\theta}\left\{\left(\frac{w_0}{w(Z_{r(l)})}\right)^{1/4} \exp\left[\frac{-X_{r(l)}^2}{w^2(Z_{r(l)})}\right]\right\} \exp[-j\beta Z_{r(l)}] \ . \qquad (15)$$

As an example, $X_{r(l)}$ and $Z_{r,l}$ for the case that there is only one reflection with considering the Goos-Hänchen shift are given by

$$Z' = \left| z\cos\theta + ((-1)^i d + \delta_\theta + W - x)\sin\theta) \right| \quad , \qquad (16)$$

$$X' = \left| (d + (-1)^i (W + \delta_\theta) + (-1)^{i+1} x)\cos\theta + (-1)^{i+1} z\sin\theta \right| \ , \qquad (17)$$

$$Z'' = \left| z\cos\theta - ((-1)^{i+1} d + (W + \delta_\theta) + x)\sin\theta \right| \quad , \qquad (18)$$

$$X'' = \left| ((-1)^{i+1} d + W + \delta_\theta + x)\cos\theta + z\sin\theta \right| \quad . \qquad (19)$$

In above relations $i = 1,2$ is denoting the number of access waveguides.

4. Calculation of the coupling coefficients

It is important to note for the case of long-length MMI domains, which is analyzed by sinusoidal model, the radiative modes are omitted and only guided modes are considered. But in analysis of small-length MMI coupler, with the Gaussian model, due to the small length of the device, there is a few reflections for each mode and therefore, a large amount

of power of every mode reaches the output waveguides. In other words, in Eq. 1 for the Gaussian model unlike the sinusoidal model we have a continuum set of Gaussian modes (all of modes with angle θ that is included in ν):

$$\psi(x,0) = \int c_{\nu,d}\,\varphi_{\nu,d}(x,0)\,d\nu \tag{20}$$

The mode-profile for the input and output waveguide are obtained by EIM method:

$$E_{\text{in}}(x,z) = E_{0,\text{in}}\cos[k_x(x-d)+\Phi_0]\exp[-j(\beta_{\text{in}}z)] \quad , \tag{21}$$

$$E_{\text{out}}(x,z) = E_{0,\text{out}}\cos[k_x(x+d)+\Phi_0]\exp[-j(\beta_{\text{in}}z)] \ . \tag{22}$$

The excitation coefficients of the modes for both the models can be determined by evaluating the longitudinal and transversal excitation coefficients [Mahmoodi, A. et al. (2009)]:

$$c_\nu = C_{\text{longitudinal},\nu}C_{\text{transversal},\nu} \quad . \tag{23}$$

The transversal excitation coefficients can be obtained by using the overlap integrals between the input field profile $(E_{\text{in}}(x,0))$ and the profile of the ν^{th} mode $(\varphi_{\nu,d}(x,0))$:

$$C_{\text{transversal},\nu} = \frac{\int \varphi^*_{\nu,d}(x,0)E_{\text{in}}(x,0)\text{d}x}{\left[\int\left|\varphi_{\nu,d}(x,0)\right|^2\text{d}x\int\left|E_{\text{in}}(x,0)\right|^2\text{d}x\right]^{1/2}} \quad . \tag{24}$$

Also, the longitudinal excitation coefficients can be obtained using the phase-matching integral along the *z* propagation:

$$C_{\text{longitudinal},\nu} = \frac{2}{T}\int_0^T \cos(\beta_{\text{in}}z)\cos(\beta_\nu z)\text{d}z\,, \tag{25}$$

where $T = 2\pi/\beta_{\min}$ and $\beta_{\min} = \min(\beta_{\text{in}},\beta_\nu)$. By normalizing the excitation coefficient c_ν as $C_\nu = c_\nu / \left|\sum_\nu c_\nu\right|$ and evaluating an overlap integral between the profile of a cross output waveguide and the mode fields of the MMI region we have:

$$E_{0,\text{cross},\nu} = C_\nu \frac{\int \varphi_\nu(x,L)E^*_{\text{out}}(x,L)\text{d}x}{\left[\int\left|\varphi_{\nu,d}(x,L)\right|^2\text{d}x\int\left|E_{\text{out}}(x,L)\right|^2\text{d}x\right]^{1/2}} C_{\text{longitudinal,cross},\nu} \ , \tag{26}$$

So, the coupling coefficient of the MMI coupler that is the ratio of the output field amplitude to the input field amplitude is determined as:

$$K = \sum_\nu E_{0,\text{cross},\nu} \ . \tag{27}$$

5. Comparison of Gaussian and Sinusoidal models

In this section, we compare Gaussian model and the sinusoidal model to become distinct their operation limits. To do this, the coupling coefficients of MMI couplers (with small lengths) for Gaussian and sinusoidal models by using the transversal and longitudinal overlapping integrals computed and are shown in Fig. 3. The parameters of MMI coupler used in this work are: $n_1 = 1.5$, $n_2 = 1.0$, $W = 6\mu m$, $h = 0.5\mu m$ and $\lambda_0 = 1.55\mu m$.

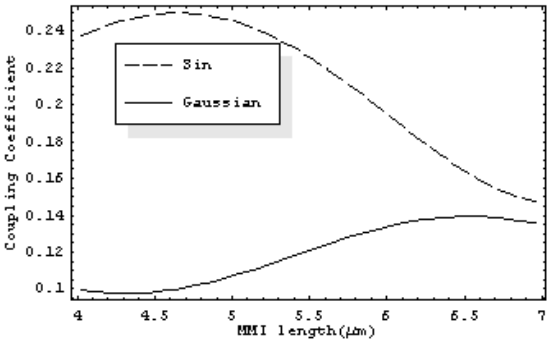

Fig. 3: The coupling coefficients of the MMI coupler for Gaussian and sinusoidal models with Goos-Hänchen shift consideration, ($d = 1\mu m$).

It must be noted that the Goos–Hänchen shift for two models are also considered. The solid line refers to the Gaussian model and the dashed line refers to the sinusoidal model. It is evident from the figure that there is a difference between the results of these models in these length ranges. This difference between the two curves shows that the only one of these models can be applied for small lengths. In fact, the results of the Gaussian model are true for small lengths and sinusoidal model cannot be used for these length ranges. To prove this, the theoretical light intensity patterns are presented in a multimode waveguide. Fig. 4(a) is obtained by using the Gaussian model, Fig. 4 (b) is the result of a simulation with FEMLAB software (FE method) [FEMLAB, Version 3.1(2004)] and Fig. 4(c) is the result of a simulation with FDTD method [Hagness, S. C. (1997)]. Because all of these light intensity patterns are identical and there is a proper accordance between them, it is evident that the theory of Gaussian model is accurate for MMI couplers with small length. The employment of sinusoidal model in analysis of light propagation for MMI coupler with short length causes poor results. This is due to the fact that building-up of sine modes is the result of multiple interferences of the reflected waves that appear in larger lengths.

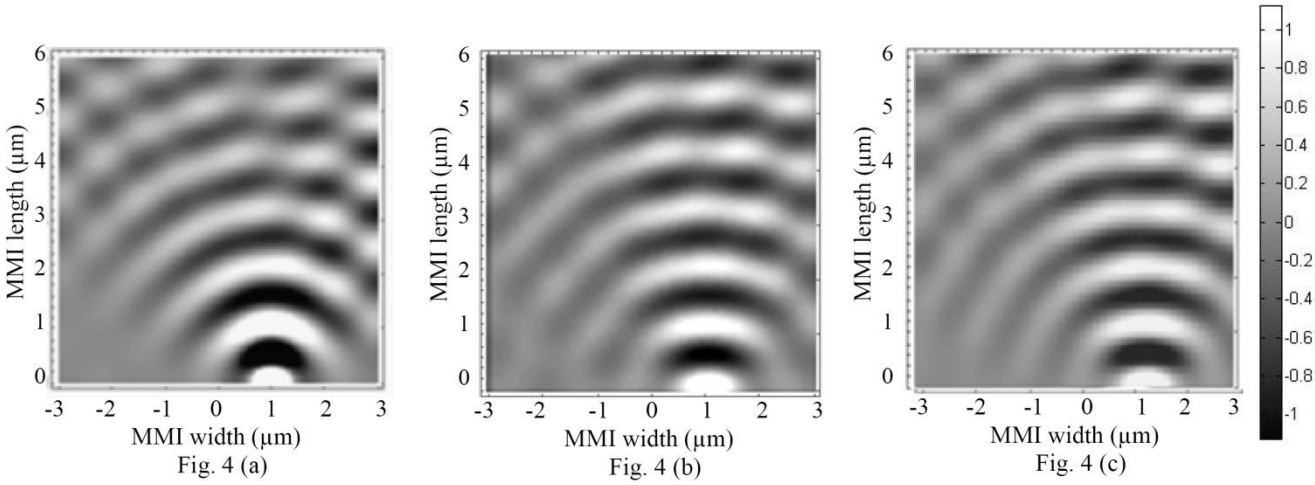

Fig. 4: comparison of light intensity pattern obtained by Gaussian model with those of simulation results. (a) is the result of Gaussian model, (b) simulation results by FEMLAB software,(c) simulation result by FDTD method.,(with Goos-Hänchen shift consideration). as [Mahmoodi, A. et al. (2009)].

In other words, the self-imaging property that is related to the interference of several modes in MMI region is based on several reflections of the wave along the region, but in short MMI waveguides there is only one or a few reflections. The theoretical light intensity patterns in a MMI region with the length greater than $10\mu m$ is shown in Fig. 5.

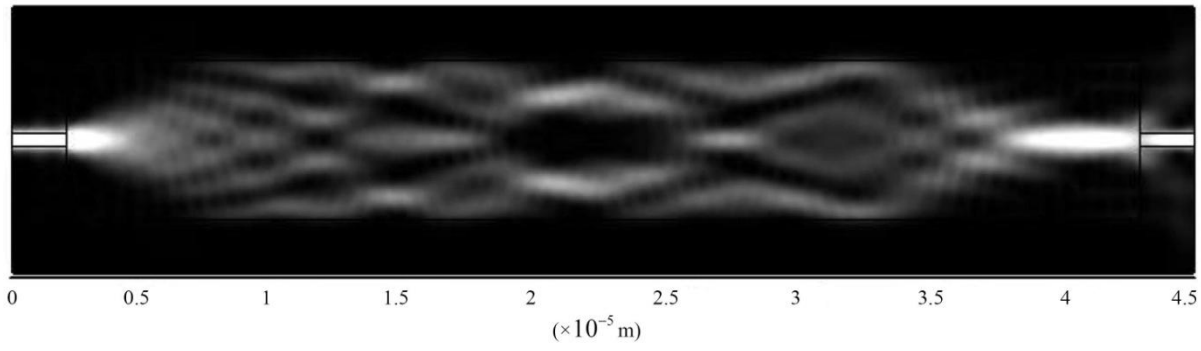

Fig. 5: Light intensity pattern in MMI region with the length greater than $10\mu m$ ($d = 2\mu m$). with Goos-Hänchen shift consideration.

At the beginning of the coupler the interference and self-imaging is not seen, but in large distances interference and self-imaging can be easily found. In fact, in long multimode waveguides, the Gaussian modes are gradually transformed into the sinusoidal modes and therefore the sinusoidal model can be used.

6. Conclusions

In this paper, the authors have presented a comparison between Gaussian and sinusoidal model of MMI coupler. The Gaussian and sinusoidal model are based on the mode propagation with Gaussian and sinusoidal eigenmodes, respectively, within the multimode region. The coupling coefficients of the MMI coupler with small length are compared for the sinusoidal and Gaussian models. Using the simulation of light intensity patterns along the length of the MMI with the FEMLAB software (based on the FE method) and FDTD method, It is confirmed that the Gaussian model is accurate for analysis of the MMI coupler with short length. Also, it is shown that for long MMI coupler due to appearance of the self-imaging, the sinusoidal model is responsible for analysis of the coupler.

Acknowledgements

The authors gratefully acknowledge the financial support of the Sama technical and vocational training college, Islamic Azad University, Karaj Branch.

References

Chang, D. C. & Kuester, E. F. (1981). A hybrid method for paraxial beam propagation in multimode optical waveguides. *Trans. Microwave Theory Technology*. 29(9). 923-933.

Davis, C.C.(1996). *Laser and Electro-Optics*. Cambridge, Cambridge University Press.

FEMLAB, Version 3.1(2004). *COMSOL Inc.*. Burlington, MA, USA.

Hagness, S.C., Rafizadeh, D., Ho, S.T., Taflove, T.(1997). FDTD microcavity simulations: Nanoscale waveguide-coupled single-mode ring and whispering-gallery-mode disk resonators. *Journal of Lightwave Technology*. 15(11), 2154–2165.

Izuka, K. (2002). Elements of Photonics, Volume II: For Fiber and Integrated optics. New York, Wiley.

Mahmoodi, A., Khanzadeh, M. and Farrahi-Moghaddam, R. (2009). Design and modeling of ultrashort MMI-based couplers. *Journal of Modern Optics*, 56(15), 1649-1658.

Marcuse, D. (1974). *Theory of Dielectric Optical Waveguides*. New York, Academic Press.

Soldano, L.B. & Pennings, E.C.M.(1995). Optical multi-mode interference devices based on self-imagings: Principles and applications. *J. Lightwave Tech.*.13(4). 615-627.

Ulrich, R. & Ankele, G. (1975). Self-imaging in homogeneous planar optical waveguides. *Applyed Physics Letter***.** 27(6).337-339.